Table 1 Sample aircraft parameters and operating data

Data item	F104-G	F-16C
C_{D0}	0.018	0.018
K	0.20	0.1326
a, rad^{-1}	2.85	3.77
S, ft^2	196	300
T, lbf	15,000	20,000
W, lbf	18,000	23,000

Table 2 Flight-path data from four sets of equations of motion

Aircraft	F104-G			F-16C		
Airspeed, ft/s	422	464	591	295	295	295
Bank angle, deg	0	30	60	0	30	60
S-4						
γ_s, deg	44.8	43.4	35.1	48.3	45.6	26.9
L_s, lbf	18,000	20,785	36,000	23,000	26,558	46,000
ρ_s, ft	NA	11,598	6,262	NA	4,696	1,566
S-3						
γ_n, deg	49.0	47.7	40.5	54.3	52.9	36.1
L_n, lbf	11,815	13,984	27,371	14,431	16,017	37,172
ρ_n, ft	NA	17,238	8,236	NA	7,787	1,937
S-2						
γ_2, deg	49.4	48.3	42.2	54.8	53.9	46.4
L_2, lbf	10,386	12,340	23,621	11,318	13,068	23,675
ρ_2, ft	NA	19,534	9,544	NA	9,545	3,042
S-1						
γ_1, deg	49.4	48.3	42.2	54.8	53.9	46.3
L_1, lbf	10,388	12,342	23,627	11,321	13,073	23,737
ρ_1, ft	NA	19,531	9,542	NA	9,541	3,034

Sample Numerical Solution Results

Two jet fighters, both at mean sea level (MSL) with flaps up, were chosen: 1) F104-G, aircraft parameters from Adamson,[2] and 2) F-16C, parameters from Asselin.[3] Details are in Table 1. Airspeeds v were picked arbitrarily but always above the relevant stall speed.

Table 2 displays solutions of the four sets of equations of motion for these two aircraft under the cited conditions, at MSL, flaps up, $\alpha_T = 0$.

Helical Flight Paths

When banked, the airplane's trajectory is a portion of a helix. To prove that fact, one can integrate approximate equations of motion either in cylindrical coordinates (carefully) or in Cartesian ones. Or, one can take a specimen helical path, parameterized by R, ω, $\dot{h} = v \sin\gamma$, and show that a mass following that path at constant speed v must be acted on by forces mirroring the equations of motion. But in fact one has no doubt that steady banked flight results in helical flight paths. The question is, Which helix?

One clue comes from the fact that the airplane's horizontal component of velocity, $v\cos\gamma$, must equal $R\omega$. In addition, we know from dynamics that $v = \rho\dot{\chi}$, and so $\rho\dot{\chi}\cos\gamma = R\omega$. One further relation is needed. Consider a coordinate system O^* parallel to our usual Cartesian system O and moving uniformly in the Z direction at speed $\dot{h}$. From the point of view of O^*, the airplane is simply moving with speed $R\omega = v\cos\gamma$ in a horizontal circle of radius R; hence, it must have force $\boldsymbol{F}^* = [m(R\omega)^2/R]\hat{\boldsymbol{n}} = [m(v\cos\gamma)^2/R]\hat{\boldsymbol{n}}$ acting on it. But because O^* is not accelerated with respect to O, $\boldsymbol{F}^*$ must equal the force as seen from the O system, $\boldsymbol{F} = (mv^2/\rho)\hat{\boldsymbol{n}}$. Hence,

$$\rho = R/\cos^2\gamma \tag{32}$$

Then from the earlier relation one finds

$$\dot{\chi} = \omega\cos\gamma \tag{33}$$

so that always $\rho > R$ and $\dot{\chi} < \omega$, as makes intuitive sense.

Conclusions

In a specific case in which one questions validity of the small flight-path angle approximation (set S-4), several analytical or numerical procedures stand ready to settle that question and, if necessary, to supplant that inadequate approximation. Set S-3 gave markedly better results than S-4 with very little additional effort. Set S-2, though yielding a more complicated quadratic, gave results almost as good as the exact numerical solutions to set S-1. Once set up, even that last procedure takes only a few minutes. The confusing relations between radii of curvature and angular speeds, looked at from the alternative aircraft dynamics and helix kinematics points of view, were clarified.

References

[1]Kerber, L. V., "Airplane Performance," *Aerodynamic Theory*, Vol. V, edited by W. F. Durand, Dover, New York, 1935, p. 254.

[2]Adamson, J. C., *Aircraft Performance M.E. 481*, U.S. Military Academy, West Point, NY, undated, p. D-2.

[3]Asselin, M., *An Introduction to Aircraft Performance*, AIAA, Reston, VA, 1997, p. 333.

Radar Cross Section Constraints in Flight-Path Optimization

Martin Norsell*
Royal Institute of Technology, SE-100 44 Stockholm, Sweden

Introduction

THE Department of Aeronautics at the Royal Institute of Technology has for some time been involved in developing methods for aircraft trajectory optimization. The optimized trajectories have been flight tested by the Swedish Air Force using the supersonic Saab J35 Draken and the jet trainer Saab 105 (Ref. 1–4).

Radar is the only threat against aircraft considered in this study. The detection time is defined as the time interval between the instant at which the aircraft is first detected and the instant at which the aircraft reaches the specified target. The detection distance is the distance from the target to the position at which the aircraft is first detected by radar. Given an initial aircraft position and a target position, the offset distance is defined as the perpendicular distance to an alternative flight path parallel to the original flight path. Hence, a flight path pointing directly at, or above, the target is defined to have zero offset.

In a previous study substantial decrease in detection time was experienced and verified in flight tests. This was achieved without any optimization methods applied.[5] The purpose of the present study is to develop a radar cross section (RCS) constraint suitable for three-dimensional flight-path optimization. To be computationally efficient, such an RCS representation has to be continuous and differentiable. To gain understanding of the potential decrease in detection time, numerical examples are considered.

Performance Model

Flight-path optimization is often performed in two dimensions, only considering the longitudinal degrees of freedom. Such a model is not suitable when RCS properties are considered because the RCS can fluctuate significantly even for small changes in pitch and bank angles.[6] The full-blown six-degree-of-freedom (6-DOF) model is

Received 3 October 2002; revision received 29 October 2002; accepted for publication 30 October 2002.

*Ph.D. Student, Department of Aeronautics. Member AIAA.

known to be computationally intense, and hence, a simplified flight mechanics model is used.[3,4] The full 6-DOF model as described by, for example, Etkin and Reid[7] is reduced, as derived by Ringertz,[4] to

$$m\dot{V} = T\cos(\alpha+\epsilon) - D - mg\sin\gamma \tag{1}$$

$$mV\dot{\gamma} = T\sin(\alpha+\epsilon)\cos\phi + L\cos\phi - mg\cos\gamma \tag{2}$$

$$mV\dot{\psi}\cos\gamma = T\sin(\alpha+\epsilon)\sin\phi + L\sin\phi \tag{3}$$

$$\dot{h}_g = V\sin\gamma \tag{4}$$

$$\dot{m}_f = -b \tag{5}$$

$$\dot{x}_1 = V\cos\gamma\cos\psi \tag{6}$$

$$\dot{x}_2 = V\cos\gamma\sin\psi \tag{7}$$

where m is the mass of the aircraft, V velocity, T thrust, α angle of attack, L lift, D drag, m_f fuel mass, and g gravitational acceleration.[4,7] Furthermore, γ is the flight-path angle, b the fuel burn, and ϵ angle of the engine thrust relative to the body-fixed coordinate system. In the Earth-fixed coordinate system, x_1 is the distance in the east direction and x_2 the distance in the north direction. The geodetic altitude h_g completes the right-hand coordinate system. The heading angle is represented by ψ, defined as zero in the x_1 direction and positive counterclockwise. Finally, the bank angle ϕ is defined as the angle of roll displacement around the velocity vector with wings level defining $\phi = 0$.

Brief Introduction to Trajectory Optimization

The method follows the methodology outlined by Ringertz.[4] One vector with state variables is formed as $\boldsymbol{x} = (V, \gamma, \psi, h_g, m_f, x_1, x_2)^T$ and another vector with the control variables as $\boldsymbol{u} = (\alpha, \phi, \delta_t)^T$ where δ_t is the thrust setting. Now the equations of motion (1–7) can be rewritten as

$$\dot{\boldsymbol{x}} = f(\boldsymbol{x}, \boldsymbol{u}) \tag{8}$$

Further algebraic constraints on dynamic pressure, load factor n_z, radar detection, and similar parameters can be written as

$$\underline{g} \le g(\boldsymbol{x}, \boldsymbol{u}) \le \bar{g} \tag{9}$$

where $\underline{g}$ and $\bar{g}$ are lower and upper bounds, respectively. The state variables are represented by piecewise cubic polynomials and the control variables by piecewise linear functions. This makes it possible to discretize Eqs. (8) and (9) using Hermite-Simpson collocation (see Ref. 8). Finally, a vector $\boldsymbol{y}$ is created, which contains the discretized state and control variables. An objective function f_0 can be formulated as, for example, flight time, detection time, or similar parameters. The optimization problem can be posed as

$$\min_{y} f_0(\boldsymbol{y}) \tag{10}$$

subject to

$$\underline{\boldsymbol{l}} \le \begin{pmatrix} c(\boldsymbol{y}) \\ C\boldsymbol{y} \\ \boldsymbol{y} \end{pmatrix} \le \bar{\boldsymbol{u}} \tag{11}$$

where $c(\boldsymbol{y})$ are the discretized state and algebraic constraints, $\underline{\boldsymbol{l}}$ the lower bounds, and $\bar{\boldsymbol{u}}$ the upper bounds. The matrix C defines the linear constraints needed to connect different stages. The different stages may involve various sets of state and algebraic equations.

Radar Range Constraint

To avoid radar detection, it is only necessary to have sufficiently low RCS, so that the echo returned is below the detection threshold of the radar.[6] The basic radar range equation can be split into two separate parts, one radar dependent ν_0 and another dependent of the aircraft RCS denoted σ, giving[9]

$$R_d = \nu_0\sigma^{\frac{1}{4}} \tag{12}$$

where R_d is the detection range. The aircraft RCS depends on the orientation of the aircraft relative to the radar station. Because σ can vary several orders of magnitude for very small variations in angle, it is important to model both the aircraft position and the attitude angles. Although it may be possible to find an exact representation of the RCS, this may not be very useful in optimization because an aircraft will always experience turbulence and other disturbances in flight.

In this study, the RCS is represented by a spline approximation. Although the RCS around an airplane is truly three dimensional, it may be reduced to two dimensions using θ_r and κ_r denoting the angle of elevation and azimuth, respectively. The RCS data can be given on a rectangular grid, defined in elevation and azimuth. The calculated RCS corresponding to the points directly above and below the aircraft, $\theta_r = \pm 90$ deg are denoted poles. It is important to assign a unique value of the RCS at the poles and to keep the grid rectangular, if a spline representation is to be calculated.[10,11]

In the optimization, a lot of function evaluations including the RCS calculation are performed that makes splines very suitable for this purpose. The derivatives at the poles are specified to be zero. Likewise, the derivatives for $\kappa_r = 0$ and 360 deg are fixed at zero, and their values are specified to be equal for continuity.

To obtain the algebraic constraint needed in optimization, the distance to the radar station has to exceed the maximum detection range governed by Eq. (12) resulting in

$$R_d^2 - (x_1 - x_{1r})^2 - (x_2 - x_{2r})^2 - (h_g - x_{3r})^2 \le 0 \tag{13}$$

where the aircraft coordinate system is defined as per Etkin and Reid and the subscript r is used to denote the radar coordinates.[7]

If there are more than one radars present, the extra constraints are simply added considering new positions, x_{1r}, x_{2r}, and x_{3r}, and R_d for any additional threats. To model the radar-dependent parameter ν_0, the direction from the radar station to the aircraft in the radar coordinate system is described by the two angles μ and η, where μ is the azimuth and η the elevation for the radar station. Furthermore, to model the aircraft-specific parameter σ a unit vector $\hat{\boldsymbol{x}}_e$ describing the direction from the aircraft to the radar station in the Earth-fixed coordinate system is introduced. The unit vector $\hat{\boldsymbol{x}}_e$ is now rotated into the body-axis system; for example, see Stevens and Lewis using the rotational matrices L_{bw} and L_{we} such that[12]

$$\hat{\boldsymbol{x}}_b = L_{bw}L_{we}\hat{\boldsymbol{x}}_e \tag{14}$$

Now the angles to the radar station in the body coordinate system can be calculated. To achieve computational efficiency, it should be possible to calculate the Jacobian of the RCS constraint without using finite differences. This is possible by differentiation of the RCS and using that $\partial\sigma/\partial\theta_r$ and $\partial\sigma/\partial\kappa_r$ are available with little additional computational effort from the spline representation.[11,13] Finally, because $\hat{\boldsymbol{x}}_e = \hat{\boldsymbol{x}}_e(x_1, x_2, h_g)$, $L_{bw} = L_{bw}(\alpha, \beta)$, where β is the angle of sideslip and $L_{we} = L_{we}(\gamma, \psi, \phi)$, the differentiation of the Jacobian used in optimization is straightforward.

Numerical Simulation

To investigate the proposed RCS constraint, a simple example is implemented and tested. The task is to start from a state when flying straight and level at 1-km altitude to a radar station located 40 km to the east and 40 km to the north. Furthermore, the flight trajectory is specified to pass the radar station at 2-km altitude. Finally, an altitude restriction of maximum 5 km is enforced. The aircraft model used describing the jet trainer Saab 105 was developed by Ringertz in a previous project.[2] In the current implementation, there are additional

algebraic constraints on the dynamic pressure, the load factor and radar detection. In the simulation, the properties of the radar station are deliberately left out. The radar range ν_0 is assumed constant, which makes the detection distance, of a target with constant RCS, a cylinder centered around the radar station. This is performed to simplify visualization. The nominal detection distance for an aircraft with an RCS of 1 m^2 is fixed to 15 km.

Generally, the RCS of the aircraft depends on both the azimuth and the elevation toward the radar station. When the aircraft approaches the radar station with some offset, the azimuth and elevation both change continuously, resulting in large fluctuations of the RCS. Most conventional airplanes, such as the Saab 105, have high RCS straight ahead due to the large radar reflections caused by the engine intakes. This is the primary cause for the long detection distance when approaching a radar station head-on. Furthermore, the wings interact with the fuselage as dihedrals, which are known to give strong RCS contributions.[6] Finally, a conventional aircraft has high RCS if spotted by a radar directly from above or below.

The RCS model used in the current implementation is a generic RCS model of a small conventional airplane. The RCS is 12.0 m^2 in the nose direction. This makes the detection distance 27.9 km if the aircraft is heading directly at the radar station.

For verification purpose, the minimum flight time and the maximum remaining fuel cases were calculated.[4] The optimization is divided in two stages, with constraints on the RCS according to Eq. (13) during the first stage and no RCS constraint during the second stage.

First the objective is to minimize the flight time during the second stage, which equals the detection time. The resulting flight path is shown in Figs. 1 and 2. The results are summarized in Table 1. Note that the aircraft is at the maximum allowed altitude for quite some time to gain maximum potential and kinetic energy before it dives for the final destination. The aircraft turns to avoid exposing its strong head-on RCS aspect, which would make it visible approximately at the distance denoted by the dash–dotted line in Fig. 2. Hence, it approaches the minimum detection distance possible denoted by the dashed line. This line corresponds to the minimum RCS in the forward aspects of the airplane. The actual RCS value is 1.4 m^2 at $(\kappa_r, \theta_r) = (37.5, 17.5)$ deg in the spline representation used. However, the total distance the aircraft flies is quite long, and this is most probably caused by the objective function only considering the detection distance and only involving the aircraft behavior during the second stage when the aircraft is already detected by the radar. It is apparent that an objective function only considering aircraft states during parts of the aircraft trajectory may be insufficient. Hence, an alternate objective is considered,

$$f_{\text{obj2}} = \min K_1 t_d + (1 - K_1)(-m_{f,\text{stage1}}) \tag{15}$$

where t_d is the detection time, $m_{f,\text{stage1}}$ the remaining fuel after the first stage, and K_1 a parameter such that $0 \leq K_1 \leq 1$. However,

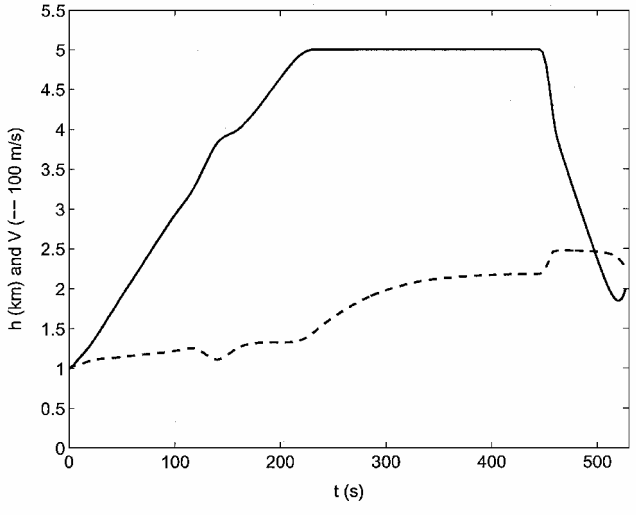

Fig. 1 Height and velocity profile; objective: minimum detection time.

Table 1 Comparison between results for different objective functions

Objective	Total time, s	Detection time, s	Fuel consumption, kg
Minimize total time	299.5	144.3	64.9
Maximize remaining fuel	462.4	236.6	46.4
Minimize detection time, $K = 1.00$	526.8	69.3	92.3
Weighted detection/fuel, $K = 0.98$	496.3	67.9	87.2
Weighted detection/fuel, $K = 0.03$	377.2	84.8	54.2

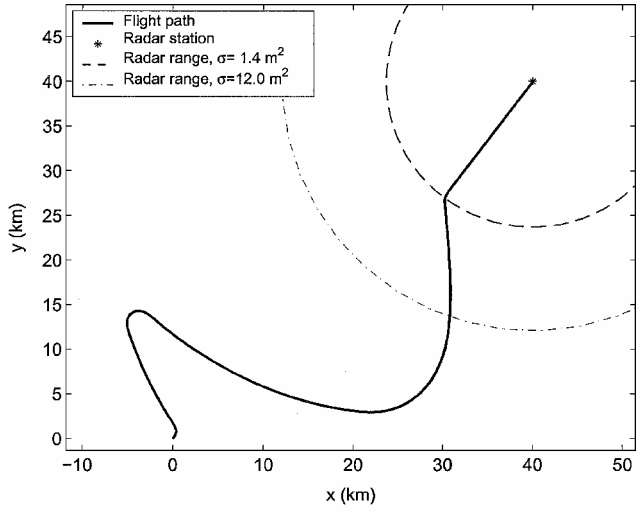

Fig. 2 Optimized trajectory in the *xy* plane; objective: minimum detection time.

the effect of K_1 on the optimization is in general dependent on the scaling of the different parts of the objective function in Eq. (15).

The same case as before is considered with the new objective function. First the value of the weight K_1 is set to 0.03, and the results are shown in Table 1. When this flight path is used, the aircraft is at the maximum altitude during a shorter time period and approaches the radar station more directly, decreasing the fuel consumption. The detection time is increased by 22% compared to the case of minimizing the detection time only. However, the aircraft spends less total time in the air, which is beneficial if there are other threats present. This implies that some kinds of robustness criteria have to be considered in the future. Finally, the weight K_1 is set to 0.98, and the fuel consumption decreases compared to the case of minimizing the detection time only. More interesting is the detection time, which actually decreases. This is most likely due to the strong nonlinearity of the optimization problem, which makes it impossible to know that the global minimum is found. However, all of the tested cases in Table 1 are much better, from a detection time point of view, than just approaching the radar station head-on. When the results in Table 1 are compared, it can be concluded that the minimum detection time for this particular case is slightly effected by limiting the fuel consumption during the first stage, but the total flight time decreases drastically. Finally, it can be concluded that, even if the global optimal flight path is not found, substantial reductions in radar detection time can be achieved.

Conclusions

The most important conclusion of the present study is that it seems possible and beneficial to use flight-path optimization with RCS constraints in three dimensions. The methods presented show potential decrease in the time an aircraft is detected by radar, when implemented and used in a simple numerical example. For more robust flight-path optimization, the RCS description has to be reasonably smooth. An exact RCS description may be desired, but is known to vary several orders of magnitude for small angular changes. This

introduces, for example, many local minima in the numerical optimization and extreme sensitivity to flight-path perturbations. In flight, all aircraft experiences such perturbations caused by, for example, turbulence. Hence, the modeling of the RCS has to be further investigated and compared to measurements.

It is concluded that, even if the global optimal flight path is not found, substantial reductions in radar detection time can be achieved. Finally, it is concluded that the objective function as well as the robustness need improvement.

Acknowledgments

This project is financially supported by the Swedish Defence Materiel Administration in a project monitored by Staffan Lundin, Curt Eidefeldt, Martin Näsman, and Bertil Brännström. The author is most grateful for the support provided by Ulf Ringertz at the Royal Institute of Technology.

References

[1]Ringertz, U. T., "Multistage Trajectory Optimization Using Large-Scale Nonlinear Programming," Dept. of Aeronautics, TR 99-25, Royal Inst. of Technology, Stockholm, Sweden, Sept. 1999.

[2]Ringertz, U. T., "Aircraft Trajectory Optimization as a Wireless Internet Application," Dept. of Aeronautics, TR 2000-11, Royal Inst. of Technology, Stockholm, Sweden, Aug. 2000.

[3]Ringertz, U. T., "Flight Testing an Optimal Trajectory for the Saab J35 Draken," *Journal of Aircraft*, Vol. 37, No. 1, 2000, pp. 187–189.

[4]Ringertz, U. T., "An Optimal Trajectory for a Minimum Fuel Turn," *Journal of Aircraft*, Vol. 37, No. 5, 2000, pp. 932–934.

[5]Norsell, M., "Flight Testing Radar Detection of the Saab 105 in Level Flight," *Journal of Aircraft*, Vol. 39, No. 5, 2002, pp. 894–897.

[6]Jenn, D. C., *Radar and Laser Cross Section Engineering*, AIAA Educational Series, AIAA, Washington, DC, 1995, Chaps. 1–2.

[7]Etkin, B., and Reid, L. D., *Dynamics of Flight, Stability and Control*, Wiley, New York, 1996, Chap. 4.

[8]Brenan, K. E., "Differential-Algebraic Equations Issues in the Direct Transcription of Path Constrained Optimal Control Problems," Aerospace Rept. ATR-94(8489)-1, The Aerospace Corp., El Segundo, CA, 1993.

[9]Paterson, J., "Overview of Low Observable Technology and Its Effects on Combat Aircraft Survivability," *Journal of Aircraft*, Vol. 36, No. 2, 1999, pp. 380–388.

[10]Newman, W. M., and Sproull, R. W., *Principles of Interactive Computer Graphics*, McGraw–Hill, New York, 1981, Chap. 21.

[11]Nilsson, U., "B-Spline Based Aerodata Model for the SK60," M.S. Thesis 99-35, Dept. of Aeronautics, Royal Inst. of Technology, Stockholm, Sweden, 1999.

[12]Stevens, B. L., and Lewis, F. L., *Aircraft Control and Simulation*, Wiley New York, 1992, pp. 37, 63.

[13]De Boor, C., "Package for Calculating with B-Splines," *SIAM Journal on Numerical Analysis*, Vol. 14, No. 3, 1997, pp. 441–472.